Received: 14 April 2022 | Revised: 19 May 2022 | Accepted: 27 June 2022

DOI: 10.1002/jcc.26967

RESEARCH ARTICLE

Journal of COMPUTATIONAL CHEMISTRY WILEY

Conformational distributions of helical perfluoroalkyl substances and impacts on stability

Maleigh Mifkovic | Daniel J. Van Hoomissen | Shubham Vyas

Department of Chemistry, Colorado School of Mines, Golden, Colorado, USA

Correspondence
Shubham Vyas, Department of Chemistry, Colorado School of Mines, 1012 14th Street, Golden, CO 80401, USA.
Email: svyas@mines.edu

Abstract

Per- and polyfluoroalkyl substances (PFAS) have been widely used the past 70 years in numerous applications due to their chemical and thermal stability. Due to their robust stability, they are environmentally recalcitrant which made them one of the most persistent environmental contaminants. In addition to strong C—F bond strength, oleophobicity, hydrophobicity, and high reduction–oxidation (redox) potential of PFAS has led to their inefficient degradation by traditional means. A characteristic of their structure is also their preference to adopt helical conformations along the carbon backbone, contrary to their hydrocarbon analogues. This work investigates the helical nature of perfluoroalkanes through their conformational distributions, especially as a benchmark for determining the impact of polar head groups, heteroatoms, and radical center on helical conformations. Since structure governs reactivity and molecular properties, it is important to assess if minor chemical perturbations in the structure will lead to changes in the conformations. Based on density functional theory calculations and comprehensive conformational distributions, it was concluded that the helicity is a local structural property which changes significantly with the presence of heteroatoms in the perfluoroalkyl chain as well as with the presence of radical centers.

KEYWORDS
conformational distributions, DFT, helicity, PFAS

1 | INTRODUCTION

Per- and polyfluoroalkyl substances (PFAS) are fully and partially fluorinated molecules, respectively, which have been employed in numerous applications such as firefighting foams,[1] lubricants,[2] and food cookware[3] throughout the past 70 years. However, these compounds have become contaminants of concern due to their recalcitrant nature and ubiquitous presence in the global ecosystem.[4,5] The robust chemical framework of PFAS has been attributed to a high C—F bond strength (131 kcal mol^{-1}),[6] inability to be easily oxidized, and their oleophobicity and hydrophobicity, all of which makes them resistant to high energy degradation techniques.[7] The most widely discussed PFAS in the literature, perfluorooctanoic acid (PFOA), and perfluorooctanoic sulfonate (PFOS), are considered substances of high concern and are regulated in both the United States and foreign countries.[8] Because of their recalcitrance and accumulation in the environment, understanding why these molecules are so robust and how their structures are impacted by different factors is important in understanding their environmental fate and transport.

It is a generally accepted notion that structure of a molecule can impact its reactivity and properties. An interesting characteristic of PFAS that may contribute to their robustness is their helical conformations. Qualitatively, helicity is described as the twisting of the carbon backbone to achieve the most stable, minimum energy structure.[9–11] Quantitatively, the average F—C—C—F dihedral angle in perfluoroalkyl chain is around 165°, contrary to hydrocarbons, which do not exhibit helicity and instead adopt an all trans structure with an anti H—C—C—H dihedral angle of 180°.[12] The source of helicity in

perfluoroalkanes (PFAs) has been investigated using computational methods in the literature. Jang et al. determined electrostatic repulsion, not van der Waals forces, between fluorine atoms as the source of these helical conformations.[13] Contrary to this, Cormanich et al. cited hyperconjugation as the origin in longer chain PFAs, by analyzing natural bond orbitals (NBOs) and determining energetic stabilization through σ_{C-C} donation of electron density to σ^*_{C-F} orbitals.[14]

Although it is valuable to establish the source of helicity from a fundamental perspective, this work focuses on how the helical structure of PFAS, which may dictate molecular properties, is impacted by various structurally relevant factors. This study systematically explored the conformational distributions of PFAs compared to their hydrocarbon analogues. The distributions of PFAs were then compared to those with different polar headgroups and heteroatoms. These factors are of interest since PFOA and PFOS contain carboxylate and sulfonate functional groups, respectively, alternatives for PFAS such as GenX™ contain oxygen heteroatoms, and radicals would likely form during oxidative degradation pathways.[7,15] It is important to understand the dependence of PFA conformational distributions by different factors to elucidate how helicity attenuates or strengthens, which may impact the fate and transport of PFAS in the environment.

2 | COMPUTATIONAL METHODS

Density functional theory (DFT) calculations were carried out using Gaussian09.d software package.[16] All molecular geometries were optimized and scanned using Becke's three-parameter correlation functional with Lee–Yang–Parr exchange functional (B3LYP)[17–19] with the 6-31+G(d,p) basis set. The stationary points obtained through these calculations were characterized as minimum energy structures or transition states by the presence of zero or one imaginary vibrational modes, respectively. We determined this level of theory was appropriate to probe helical conformations when compared to others with a higher exchange and empirical dispersion corrected functionals (see Table S1). Relaxed potential energy scans were used to compute the conformational energy of all optimized structures by rotating the central F—C—C—F dihedral angle in 10° increments. All calculations were performed in the gas phase, except where the solution phase is noted. Where the solution phase calculations were performed, implicit water solvation was modeled using solvation model based on density (SMD) methodology.[20]

3 | RESULTS AND DISCUSSION

3.1 | Conformational distributions of PFAs

It is well known that the most stable structures of C2 to C6 hydrocarbons exist in all trans conformations.[12] In contrast, beginning at a C4 PFA, the minimum energy (most stable) conformations are helical, characterized by the torsional twist of the central F—C—C—F or C—C—C—C dihedral angle as shown in Figure 1. Using the F—C—C—F dihedral angle, we probed the differences of conformational distributions of C2 to C6 PFAs and their hydrocarbon analogues by analyzing their potential energy surface (PES) scans. Shown in Figure 1, the PES scans for C2 and C3 PFAs are similar to their alkane analogues with respect to *anti* (180°, minimum energy) and *eclipsed* (0°, maximum energy) conformations. However, the dihedral angle of the minimum energy structures of C4 to C6 PFAs shifts to 168° from the 180° observed in their alkane analogues, consistent with literature.[10,11,13] The differences in torsional twist of C2 and C3 PFAs compared to C4,

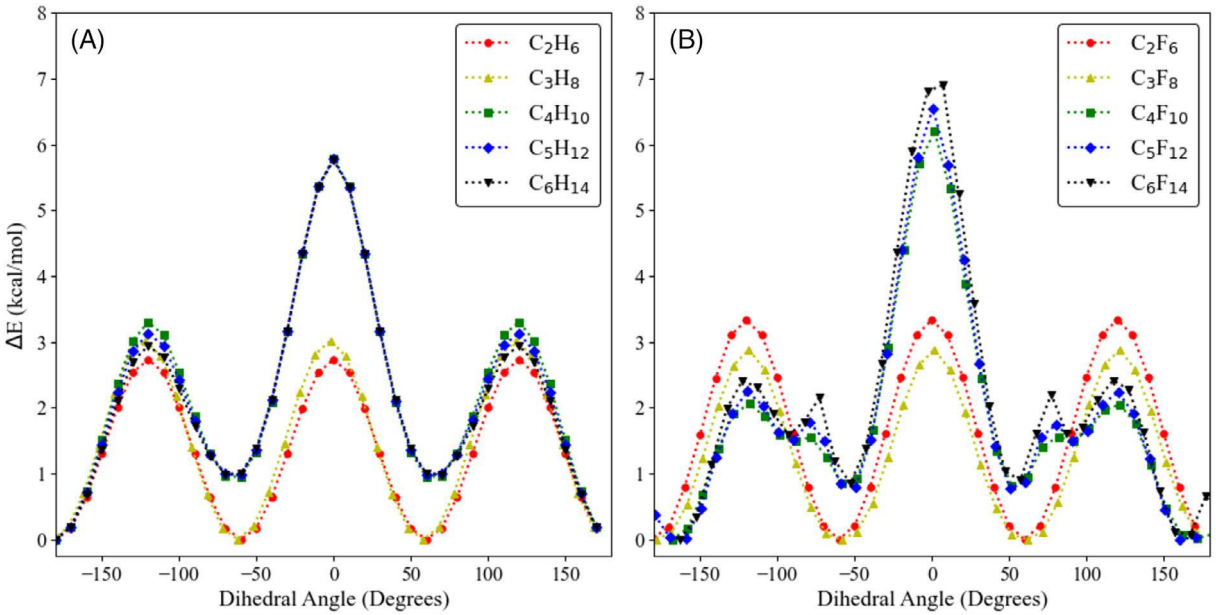

FIGURE 1 Potential energy surface (PES) scans of C2–C6 (A) hydrocarbons, and (B) PFAs as calculated using B3LYP/6-31+G(d,p) level of theory.

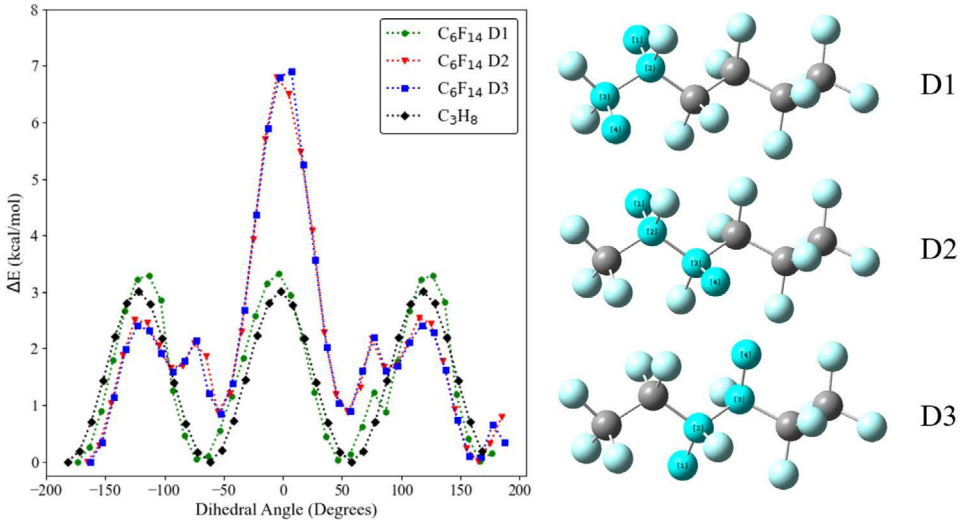

FIGURE 2 Potential energy surfaces of C6 PFA scanning three different F—C—C—F dihedral angles. D1 represents the terminal F—C—C—F dihedral, D2 represents the F—C—C—F between the terminal and central dihedral angles, and D3 represents the central F—C—C—F dihedral.

C5, and C6 can be qualitatively observed in Figure S1B. Thus, helicity begins at a C4 PFA.

The extra minima and maxima in the C4 PFA PES are confirmed by the PES scan with a smaller step size (Figure S1A). The same results (extra minima/maxima and dihedral angle shift) are observed when the central C—C—C—C dihedral angle was used for the scan in place of the central F—C—C—F dihedral angles (Figure S2). In addition, the helical nature is not impacted by dispersion corrections in the level of theory (calculated using the ωB97XD functional) (Figure S3). The causes for helical conformations have been debated in the literature, due to both F—F repulsive interactions (in short chain PFAs) as well as hyperconjugative interactions (in longer chain PFAs).[13,14] This report, however, does not focus on the source of helicity, but rather looks at the impact of polar head groups, heteroatoms, radicals, and redox processes on the helical conformations. The PESs shown in Figure 1 serve as a benchmark for a comparison with other relevant PFAS and associated intermediates discussed in the subsequent sections.

3.2 | Conformational distributions and locality of helicity

To understand how helicity depends on different dihedral angles (D), PES scans were produced against the three F—C—C—F dihedral angles for C6 PFAs, shown in Figure 2. The C6 PFA was chosen since it had the greatest torsional twist and thus the most prominent helical nature. Figure 2 shows that helicity is characterized locally and is dependent on the dihedral angle chosen. Since the PES of the terminal F—C—C—F (D1) appears more like that of C_3H_8, which is not helical, the helical nature of C_6F_{14} is not captured when the first dihedral is analyzed. Therefore, dihedral angle D1 would not be a representative choice to describe the helicity of the C6 PFA. The conformational distribution of D2 followed the same trend as that of D3 with respect to the number of observed peaks and the shift in the dihedral angle of the most stable conformation from −180° (−162° for D2 and −165° for D3). Therefore, helicity is a local attribute of PFAs, and dihedral angles chosen at or closer to the center of the molecule for the scan effectively characterize the helical nature of the molecule.

The locality of helicity was further examined in C4 to C7 PFAs by comparing the change in energy of the helical conformations with the trans conformation in which the central F—C—C—F dihedral angle is fixed at 180°. Shown in Table S2a, as chain length increases the energetic separation between the helical and trans structures increases, indicating that helicity will be stabilized in the middle of the chain and thus less prone to degradation at the center. Furthermore, the Boltzmann distribution ratios in Table S2b demonstrate that the ground state helical conformations would likely be even more prominent at room temperature than the all-trans configuration (all dihedral angles were fixed at 180°). Thus, as chain length increases, the helical conformation exclusively becomes the dominant structure (99.9% of conformations would prefer to adopt helicity for C7 PFA). Therefore, even with head groups such as carboxylates and sulfonates, which would only be on one side of the chain, these groups will likely not affect the locality of helicity. Instead, helicity is a local attribute based on chain length. Nevertheless, these functional groups are relevant regarding the two most widely discussed PFAS (PFOA and PFOS), and the impact of these groups is discussed further in the next section.

3.3 | Conformational distributions of PFAs with head groups

We probed the impact of polar head groups on helicity with perfluoroalkyl carboxylates (PFCAs) and perfluoroalkyl sulfonates (PFSAs), since these have been two of the most widely discussed classes of PFAS.[4] For PFCAs, the atom number refers to the total number of fluorinated carbons in the molecule, excluding the carbon of the carboxylic group. For example, C7 PFCA is a C6 PFA with a carboxylic acid head group (—CO_2H). Shown in Figure S4A for comparison, C3 to C7 alkyl carboxylic acid molecules do not exhibit helicity due to their all trans (180°) minimum energy structures. The PES plots of protonated PFCAs (Figure 3A) mirror the number of maxima and minima as

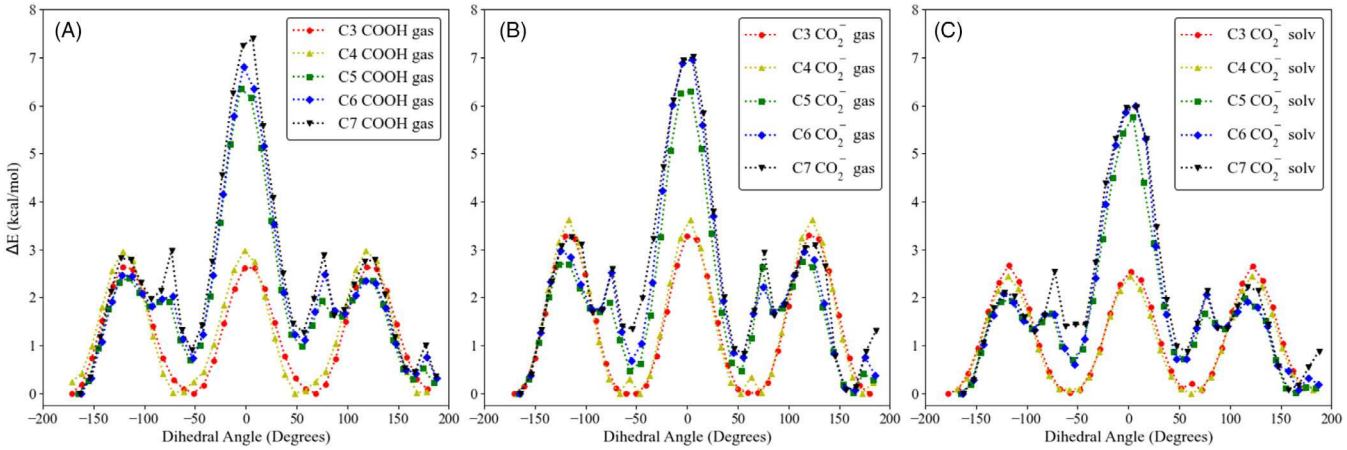

FIGURE 3 Potential energy surface plots of C3–C7 PFCAs (A) protonated in the gas phase, (B) unprotonated in the gas phase, and (C) unprotonated using implicit water solvation. All results scanned the central F—C—C—F dihedral angle. The atom number (i.e., C7) refers to the total number of carbons in the molecule.

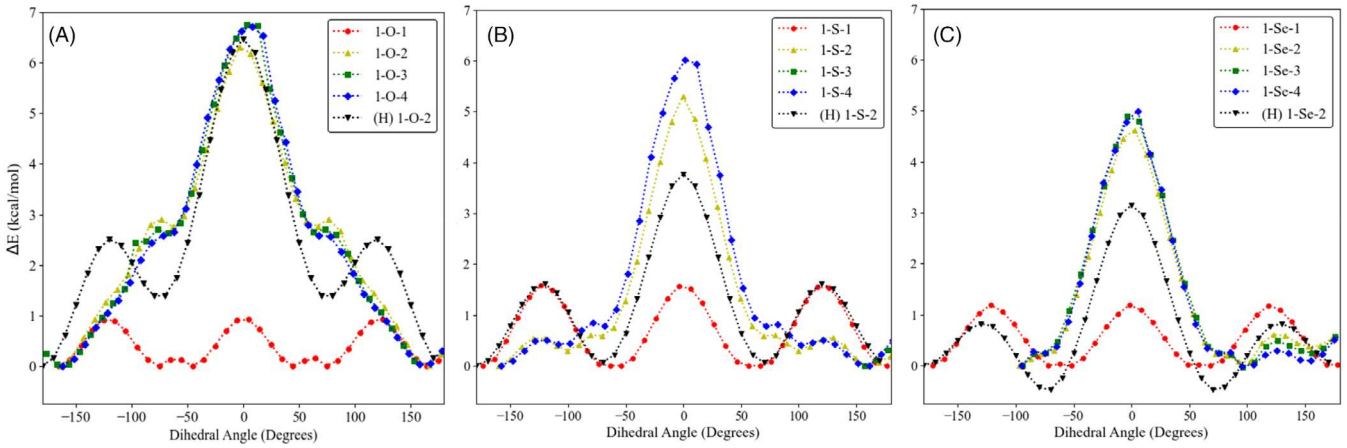

FIGURE 4 Conformational distribution plots of PFAs with (A) oxygen, (B) sulfur, and (C) selenium heteroatoms, with their 1—X—2 alkane analogue (where X = O, S, or Se) for comparison.

well as torsional twist of the minima of their corresponding PFAs (Figure 1B). PFCAs exhibit helical nature beginning at a four-carbon chain (C5 PFCA) due to the 165° dihedral angle of the lowest energy structure. This shows that the helicity does not change due to the incorporation of a polar carboxylic head group.

It is important to note that the pKa of PFCAs is significantly low and has been a subject of debate in the literature.[21,22] Nevertheless, at environmentally relevant conditions, PFCAs will be deprotonated.[5] As a result, helical conformations of deprotonated PFCAs were also explored in the gas and the solution phase (Figure 3B,C, respectively). These PFCAs were found to exhibit similar conformational distributions as their protonated forms, with slightly less energetic barriers for conformational changes. Similar conformational results were also observed for protonated PFSAs in the gas phase and unprotonated PFSAs in the gas and the solution phase (Figure S5). Therefore, helicity is not significantly affected by these protonated or unprotonated functional groups and is purely a result of the perfluoroalkyl chain.

3.4 | Conformational distributions of PFAs with heteroatoms

To replace environmentally persistent perfluoroalkyl acids, perfluoroalkyl ethers (PFAEs) such as GenX were devised, which contain an oxygen heteroatom.[23,24] We probed how helical conformations may be impacted by the placement of various heteroatoms, by computing the PES scans of C2 to C6 PFAS with oxygen, sulfur, and selenium, named O—PFAs, S—PFAs, and Se—PFAs, respectively. We refer to a molecule such as C_nF_{2n+1}—X—C_mF_{2m+1} as *n*—X—*m*, where X could be O, S, or Se, and *n* and *m* refer to the number of carbons on each side of the heteroatom. For example, CF_3—CF_2—CF_2—O—CF_2—CF_3 and CF_3—CF_2—S—CF_3 will be referred as 3—O—2 and 2—S—1, respectively.

As shown in Figure 4A, PES plots for these compounds differed slightly from their PFA analogues, namely a noticeable widening of rotational barriers. The dihedral angle of molecule 1—O—1 shifted

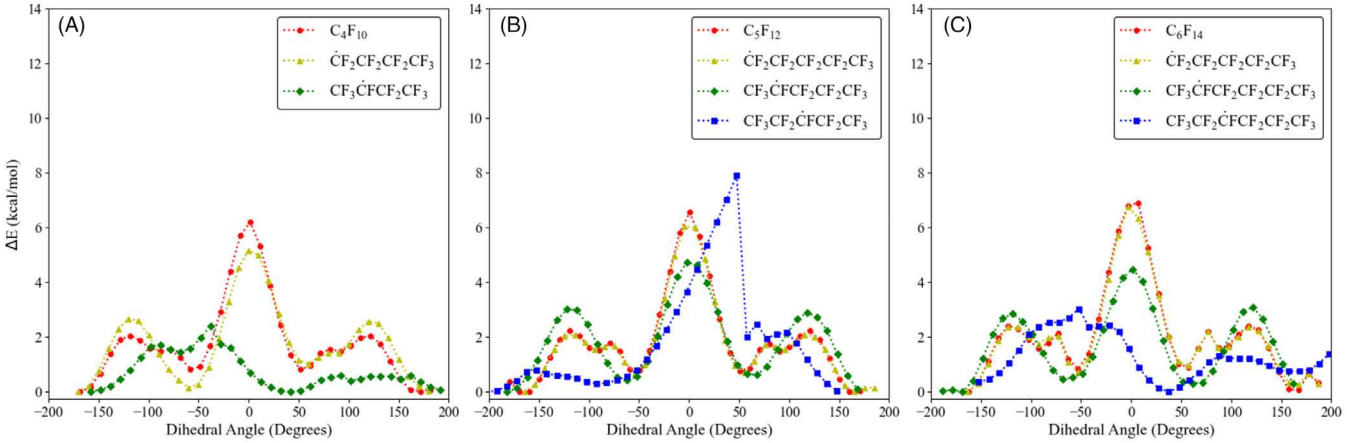

FIGURE 5 Potential energy surface scans for (A) C4, (B) C5, and (C) C6 RPFAs.

from 180° for H—C—O—C, to 166° for F—C—O—C, suggesting helical conformations are adopted in PFAEs with a backbone of three atoms (one heavy), contrary to the adoption of helicity in PFAs with a chain length of four carbons. The comparison of the distribution of 1—O—2 with that of its hydrogen analogue further indicates the adoption of helicity in a PFAE chain length of four atoms since the PES of 1—O—2 shows extra minima and maxima in addition to the shift in the dihedral angle (Figure 4A). As the chain length increases (and the oxygen is kept in the same position), the rotational barriers widen but remain relatively the same energetically. At higher temperatures, this widening may allow for greater accessibility of intermediate conformations, which has implications in reduction–oxidation and elimination degradation mechanisms.

A similar but smaller shift in the dihedral angle of the most stable structure of molecule 1—S—1 (dihedral angle = 174°) was observed (Figure 4B). Similar to 1—O—1, the deviation of the dihedral angle from 180° also indicates that 1—S—1 begins to adopt helicity. However, the lower degree of helicity in 1—S—1 was attributed to the larger size of sulfur (1.89 Å van der Waals radius) compared to an oxygen atom (1.50 Å van der Waals radius). As chain length increases, the extra minima and maxima of the conformational distributions of PFAs with sulfur heteroatoms are lower in energy compared to that of the oxygen heteroatoms. This may be due to stabilization from the larger *p* orbitals in sulfur than in oxygen, due to hyperconjugative interactions, making molecular rotations more feasible.[25]

The PES scans of PFAs with a selenium heteroatom (1—Se—2, 1—Se—3, and 1—Se—4) show that there is no chain length dependence on helicity (Figure 4C). Overall, these rotational barriers are lower in energy than the PES scans of PFAs containing sulfur and oxygen heteroatoms. Selenium also caused a significant disruption in the conformational distribution, shown by a shift in the F—C—Se—C dihedral angle of the most stable structure of 1—Se—3 to 148° (Figure S6). Longer bond lengths between the α carbon (Figure S1, inset) and selenium atom may distort the most stable conformation, allowing more rotational freedom of the methyl group. This reduces torsional twist, compared to PFAs with an oxygen heteroatom, which due to its smaller size, results in a shorter bond length and less mobility.

3.5 | Conformational distributions of radical PFAs

Perfluoroalkyl radicals (RPFAs) are intermediates during both oxidative and reductive degradations (Scheme S1).[7,15] Therefore, we calculated the PES scans of C4 to C6 RPFAs to evaluate their helical conformations and compare them against their PFA analogues. Probing helical conformations of RPFAs is more complex than PFAs, since RPFAs may undergo 1,2-F atom shifts, causing the formation of more isomers of RPFAs.[26] For example, C4 RPFAs can have the chemical structures $CF_3CF_2CF_2\dot{C}F_2$ and $CF_3CF_2\dot{C}FCF_3$, which are referred as α-C4RPFA and β-C4RPFA (Figure S1, inset).

The most notable result of the PES scan of α-C4RPFA (Figure 5A), compared to its parent PFA analogue, showed elimination of the peak at −80° in the C4 PFA PES (Figure 1). Because it is well known that alkanes adopt all-trans structures, the similarity between the potential energy scans of this RPFA with its hydrogen analogue indicated that the α-C4RPFA does not adopt a helical conformation. Comparison of the PES of C5 and C6 RPFAs with an α site radical showed similar rotational energy barriers and the same number of minima and maxima, and thus a retention of helicity (Figure 5B,C).

However, radical introduction at the β site for both C5 and C6 RPFAs show a loss in helicity, attributed to both the shift in the dihedral angle of the most stable conformation from −165° back to −180°, as well as the loss of the extra minima and maxima in the conformational distribution (Figure 5B,C). Shown in Figure S7, the PES scan of β-C5RPFA looks remarkably similar to its alkane analogue. Therefore, as the radical is introduced closer to the center of the molecule, helicity becomes disrupted and other conformations may become more energetically accessible.

4 | CONCLUSIONS

This study reports the conformational distributions of short-chain (C2 to C6) PFAs containing polar head groups (CO_2H, CO_2^-, SO_3H, and SO_3^-), heteroatoms (oxygen, sulfur, and selenium) and radicals at various sites in C4 to C6 PFAs to determine the impact of these factors on the helical nature. The calculations show that helicity is adopted at a chain length of four carbons in PFAs, with a shift in the dihedral angle of the lowest energy conformer at 168°, consistent with literature. Their conformational distributions are not affected by long-range dispersion corrections. The central F—C—C—F dihedral angle chosen for the scan shows helicity is a local characteristic within the molecule. Furthermore, helicity is not significantly affected by protonated or unprotonated functional groups and is instead a direct result of the perfluorinated chain. The addition of heteroatoms widens rotational barriers, however, larger atoms such as selenium significantly distort the lowest energy conformation, compared to oxygen and sulfur which do not. Our work also demonstrates that a radical positioned at the β site in the C5RPFA breaks helicity, shown by the similarity in its conformational distribution to its non-helical alkane analogue. Therefore, more conformations may become more energetically accessible, which is important for degradation mechanisms involving radical intermediates. Future work is needed to understand the theoretical origins of these helical conformations and determine if the helicity of PFAS can be directly correlated to the robust properties of these molecules.

ACKNOWLEDGMENTS

The financial support from National Science Foundation (CHE-1710079 and CHE-2109210) is gratefully acknowledged. The authors acknowledge the high-performance computing facility at the Colorado School of Mines for their resources.

DATA AVAILABILITY STATEMENT

Data that support this study is available as supplemental information on the journal webpage.

ORCID

Maleigh Mifkovic https://orcid.org/0000-0002-8972-3437
Shubham Vyas https://orcid.org/0000-0002-5849-8919

REFERENCES

[1] C. A. Moody, J. A. Field, *Environ. Sci. Tech.* **2000**, *34*, 3864.
[2] C. D. Vecitis, H. Park, J. Cheng, B. T. Mader, M. R. Hoffmann, *J. Phys. Chem. A* **2008**, *112*, 4261.
[3] P. J. Rae, E. N. Brown, *Polymer* **2005**, *46*, 8128.
[4] J. P. Giesy, K. Kannan, *Environ. Sci. Tech.* **2002**, *36*, 146A.
[5] R. C. Buck, J. Franklin, U. Berger, J. M. Conder, I. T. Cousins, P. de Voogt, A. A. Jensen, K. Kannan, S. A. Mabury, S. P. van Leeuwen, *Integr. Environ. Assess. Manage.* **2011**, *7*, 513.
[6] B. E. Smart, in *Organofluorine Chemistry: Principles and Commercial Applications* (Eds: R. E. Banks, B. E. Smart, J. C. Tatlow), Springer Science+Business Media, New York **1994**, Ch.3, p. 71.
[7] M. Trojanowicz, A. Bojanowska-Czajka, I. Bartosiewicz, K. Kulisa, *Chem. Eng. J.* **2018**, *336*, 170.
[8] Environmental Protection Agency (EPA), *Lifetime Health Advisories and Health Effects Support Documents for Perfluorooctanoic Acid and Perfluorooctane Sulfonate* **2016**, 81.
[9] D. A. Dixon, *J. Phys. Chem.* **1992**, *96*, 3698.
[10] W. G. Golden, E. M. Brown, S. E. Solem, R. W. Zoellner, *J. Mol. Struct.: THEOCHEM* **2008**, *867*, 22.
[11] J. A. Fournier, R. K. Bohn, J. A. Montgomery, M. Onda, *J. Phys. Chem. A* **2010**, *114*, 1118.
[12] V. Pophristic, L. Goodman, *Nature* **2001**, *411*, 565.
[13] S. S. Jang, M. Blanco, W. A. Goddard, G. Caldwell, R. B. Ross, *Macromolecules* **2003**, *36*, 5331.
[14] R. A. Cormanich, D. O'Hagan, M. Bühl, *Am. Ethnol.* **2017**, *129*, 7975.
[15] D. J. van Hoomissen, S. Vyas, *Environ. Sci. Tech. Lett.* **2019**, *6*, 365.
[16] M. J. Frisch, G. W. Trucks, H. B. Schlegel, G. E. Scuseria, M. A. Robb, J. R. Cheeseman, G. Scalmani, V. Barone, G. A. Petersson, H. Nakatsuji, X. Li, M. Caricato, A. Marenich, J. Bloino, B. G. Janesko, R. Gomperts, B. Mennucci, H. P. Hratchian, J. V. Ortiz, A. F. Izmaylov, J. L. Sonnenberg, D. Williams-Young, F. Ding, F. Lipparini, F. Egidi, J. Goings, B. Peng, A. Petrone, T. Henderson, D. Ranasinghe, V. G. Zakrzewski, J. Gao, N. Rega, G. Zheng, W. Liang, M. Hada, M. Ehara, K. Toyota, R. Fukuda, J. Hasegawa, M. Ishida, T. Nakajima, Y. Honda, O. Kitao, H. Nakai, T. Vreven, K. Throssell, J. A. Montgomery Jr., J. E. Peralta, F. Ogliaro, M. Bearpark, J. J. Heyd, E. Brothers, K. N. Kudin, V. N. Staroverov, T. Keith, R. Kobayashi, J. Normand, K. Raghavachari, A. Rendell, J. C. Burant, S. S. Iyengar, J. Tomasi, M. Cossi, J. M. Millam, M. Klene, C. Adamo, R. Cammi, J. W. Ochterski, R. L. Martin, K. Morokuma, O. Farkas, J. B. Foresman, D. J. Fox, *Gaussian 09, Revision A.02*, Gaussian, Inc., Wallingford, CT **2016**.
[17] A. D. Becke, *J. Chem. Phys.* **1993**, *98*, 5648.
[18] C. Lee, W. Yang, R. G. Parr, *Phys. Rev. B* **1988**, *37*, 785.
[19] P. J. Stephens, F. J. Devlin, C. F. Chabalowski, M. J. Frisch, *J. Phys. Chem.* **1994**, *98*, 11623.
[20] A. V. Marenich, C. J. Cramer, D. G. Truhlar, *J. Phys. Chem. B* **2009**, *113*, 6378.
[21] M. W. Sima, P. R. Jaffé, *Sci. Total Environ.* **2021**, *757*, 143793.
[22] S. Rayne, K. Forest, *J. Mol. Struct.: THEOCHEM* **2009**, *949*, 60.
[23] Z. Wang, I. T. Cousins, M. Scheringer, K. Hungerbuehler, *Environ. Int.* **2015**, *75*, 172.
[24] Z. Wang, I. T. Cousins, M. Scheringer, K. Hungerbühler, *Environ. Int.* **2013**, *60*, 242.
[25] L. Carballeira, I. Ferez-Juste, *J. Phys. Chem. A* **2000**, *104*, 9362.
[26] D. J. Van Hoomissen, S. Vyas, *J. Phys. Chem. A* **2017**, *121*, 8675.

SUPPORTING INFORMATION

Additional supporting information can be found online in the Supporting Information section at the end of this article.

How to cite this article: M. Mifkovic, D. J. Van Hoomissen, S. Vyas, *J. Comput. Chem.* **2022**, *43*(24), 1656. https://doi.org/10.1002/jcc.26967